

PORCELAIN STONEWARE VERSUS PORCELAIN: PHASE EVOLUTION, NON-CRYSTALLINE MATRIX PROPERTIES AND SINTERING KINETICS

**Chiara Zanelli¹, Sonia Conte¹, Chiara Molinari¹, Guia Guarini¹, Matteo Ardit²,
Giuseppe Cruciani², Michele Dondi¹**

¹CNR-ISTEC, Via Granarolo 64, 48018 Faenza, Italy

²Dept. Physics and Earth Sciences, University of Ferrara, Ferrara, Italy

ABSTRACT

During the various stages of ceramic tile production, sintering kinetics, phase transformations and variation of the main properties of non-crystalline matrix are considered the major parameters to be kept under control. Particularly, during the sintering process a complex evolution of both phase composition and chemistry of the liquid phase occurs, according to the dynamic equilibrium established between the residual minerals and the new crystalline phases formed during firing. This contribution aimed at comparing the evolution of phase composition and of non-crystalline matrix properties during the vitrification path of four representative industrial ceramic formulations (soft porcelain, vitreous china; two different batches of porcelain stoneware, including a glass-bearing one). These batches were designed and prepared at the laboratory scale, simulating the industrial ceramic process. The sintering kinetics of each sample was determined under isothermal conditions through an industrial-like firing schedule by optical thermo-dilatometric analysis. Samples were investigated between the temperature at which the viscous flow sintering starts (around 1000°C) up to the onset of deformation (up to 1400°C for porcelain), upon increasing dwell time. The phase composition was assessed by the Rietveld refinement and the chemical composition of the vitreous phase was obtained by subtracting the contribution of each mineralogical phase, considering its stoichiometric ideal formula.

The melt properties were estimated by predictive models based on the chemical composition of the liquid phase. An increasingly faster sintering kinetics was observed in the order: soft porcelain, vitreous china, porcelain stoneware, glass-bearing stoneware. Different vitrification paths were observed with a correlation between the dissolution kinetics of feldspar and quartz. Remarkable differences were observed in those samples where mullite occurred as primary or secondary mullite. Those differences clearly reflected a distinctive evolution of chemical features and glass network connectivity parameters of the non-crystalline matrix. The porcelain stoneware sintered by fast cycles thanks to a sort of buffering effect played by quartz and primary mullite melting rates. In contrast, vitreous china and soft porcelain needed higher temperature and/or prolonged time to activate both the growth of secondary mullite and the contemporaneous quartz dissolution, and the variation of properties of the non-crystalline matrix.

INTRODUCTION

The terms porcelain and porcelain stoneware refer to dense, light-coloured, and largely vitrified ceramic materials, which are utilized in distinct applications. Porcelain is mainly used, with its several variants, for tableware, sanitaryware, electric insulators, and art ware [1-2]. Porcelain stoneware (sometimes porcelainized stoneware) is essentially employed for wall and floor tiles, large slabs, and kitchen tops [3].

Both materials are prepared with the same ingredients (e.g., kaolin, ball clay, feldspar, quartz) but in different ratios. Porcelain batches are based on well-established technological roles of raw materials: plastic component (kaolin, ball clay); flux (potassium and mixed K-Na feldspars, nepheline syenite); filler (quartz, chamotte, alumina) [1]. For this reason, porcelain bodies are often referred to as triaxial batches [2]. Porcelain stoneware bodies are more flexible to design, and batches are usually formulated on the dichotomy between plastic (ball clay, sometimes kaolinite or pyrophyllite) and non-plastic raw materials, which are mostly fluxes: sodium and mixed Na-K feldspars, quartz-feldspathic sands, etc. [3]. Filler is added as a minor ingredient since quartz is commonly provided to some extent by fluxes and clay materials [4]. Differences in batch design reflect distinct technological requirements imposed by ceramic processing, especially in the shaping and firing stages.

Porcelain bodies are generally processed by slip casting, roll casting, or isostatic pressing [1], while porcelain stoneware tiles are manufactured by uniaxial pressing, roll compaction, or extrusion [5]. Porcelain requires firing schedules lasting several hours, typically at a maximum temperature in the 1250-1300°C range (sanitaryware), or a double-firing in the case of tableware: biscuit fired at 900-1000°C, gloss fired at 1250-1400°C [1-3,5]. In contrast, porcelain stoneware tiles are produced by fast single-firing with schedules around 1 hour cold-to-cold, extending to 2-3 hours just in case of high thickness and/or large slabs [5].

Despite the aforementioned differences, the terms porcelain stoneware and porcelain are often erroneously used as synonyms. It has become customary to shorten the term 'porcelain stoneware tiles' into 'porcelain tiles' which might cause misunderstandings. As a matter of fact, a recognized distinction in terms of composition between porcelain and porcelain stoneware is lacking, so confusion is fuelled by the absence of criteria to clearly discriminate these two materials. This circumstance may induce the questionable idea that porcelain stoneware and porcelain are just variations of the same material with a gradual change in technological behaviour and phase composition between the two end terms. To clarify this point, the present study was undertaken to understand in depth the reasons behind the different firing behaviour of triaxial batches. The goal is to unveil the microstructural mechanisms governing sintering kinetics and vitrification paths of porcelain stoneware compared with porcelain.

EXPERIMENTAL

Four batches were designed to reproduce typical industrial bodies for tableware, sanitaryware, and floor tiles. In particular, two porcelain-like materials were prepared (a soft porcelain, SOPO, and a vitreous china, VICH) together with two kinds of porcelain stoneware: a classic body (GPOR) and a glass-bearing stoneware (GSTO), to account for the possibility of recycling a glass cullet. In order to constrain the well-known effects of the Na/K ratio [6-7] and the silica content [8], all the batches were designed with the same raw materials: ball clay, kaolin, K-Na feldspar, and quartz sand (Table 1). In addition, a soda-lime glass, currently utilized in tile-making, was employed in the body GSTO. All batch chemical compositions are reported in Table 1, together with the body formulations.

wt%	Porcelain stoneware (GPOR)	Glass-bearing stoneware (GSTO)	Vitreous china (VICH)	Soft porcelain (SOPO)
Ball clay	40	40	23	-
Kaolin	-	-	27	50
Quartz	15	13	25	25
K-Na feldspars	45	27	25	25
Glass	-	20	-	-
SiO ₂	71.62	71.83	72.46	70.43
TiO ₂	0.57	0.69	0.46	0.15
Al ₂ O ₃	20.29	16.97	21.90	24.49
Fe ₂ O ₃	0.38	0.52	0.57	0.61
MgO	0.54	1.08	0.46	0.22
CaO	0.43	2.48	0.36	0.31
Na ₂ O	5.25	5.28	2.62	2.61
K ₂ O	0.92	1.16	1.17	1.18

Table 1. Batch design and chemical composition

The four batches were investigated at the laboratory scale, simulating the industrial tile-making process by: *i*) mixing and wet grinding in a porcelain jar with dense alumina media for 15min in a planetary mill; *ii*) slip drying at $105\pm 5^\circ\text{C}$, powder deagglomeration (by hammer mill) and humidification with 7–8% water; *iii*) uniaxial pressing (40 MPa) of 50mm diameter discs; drying in an electric oven at $105\pm 5^\circ\text{C}$ overnight; *iv*) firing in an electric kiln at maximum temperatures from 1000 to 1250°C with a thermal cycle of about 1h cold-to-cold. Further firings up to 1380°C were carried out for VICH and SOPO, with a slow thermal cycle of about 24h cold-to-cold. The fired products were characterized by determining the firing shrinkage, water absorption, open porosity, and bulk density (ISO 10545-3) as well as the closed and total porosity (ASTM C329).

Quantitative phase analysis (QPA) was obtained by X-ray powder diffraction (Bruker, D8 Advance Karlsruhe, Germany) using the Rietveld method as implemented in the EXPGUI-GSAS package [9-10]. All samples were admixed with corundum (20wt%) as internal standard to estimate the vitreous phase [11]. The chemical composition of the vitreous phase was calculated by subtracting from the bulk chemistry of the fired body the contribution of mineralogical phases, assuming their stoichiometric compositions weighted on the QPA. Such a vitreous phase contains different elements that affect both structure and properties of the glass network. In order to facilitate data interpretation, some parameters were used to express specific structural features of the melt:

- degree of depolymerization of the melt (NBO/T) defined as the number of Non-Bridging Oxygens (NBO) per tetrahedrally-coordinated cations (Si, Al) as atomic percentage and calculated from the composition of the vitreous phase;
- alumina saturation index of the melt $\text{ASI} = \text{Al}_2\text{O}_3 / (\text{Na}_2\text{O} + \text{K}_2\text{O} + \text{CaO})$ as molar percentage representing the amount of Al_2O_3 in the melt not provided by feldspars [7].

The physical properties of the vitreous phase at high temperature were estimated by predictive models based on the chemical composition of the liquid phase. The shear viscosity was calculated based on the Giordano and co-workers model [12], and the surface tension was estimated interpolating the data obtained by the Appen's [13] and Dietzel's [14] methods.

Moreover, the effective viscosity of the body (η_{eff}) was calculated as the product of the shear viscosity of the liquid phase (η_{melt}) by the relative viscosity (η_{rel}), i.e., $\eta_{\text{eff}} = \eta_{\text{rel}} \cdot \eta_{\text{melt}}$ [7]. The relative viscosity was estimated by the relation: $\eta_{\text{rel}} = (1-\phi)^{-B}$, where ϕ is the fraction of non-crystalline matrix and B the Einstein's coefficient [15]. The sintering behaviour was also evaluated by hot stage microscopy, using an optical thermo-dilatometer (TA, ODP868, Germany) which registered the size variation, determined by the pixel count, during the thermal cycle of specimens ($5\times 5\times 5$ mm in size) cut from the dry samples. The tests were run under isothermal conditions at the 1200°C , with a gradient of $80^\circ\text{C}\cdot\text{min}^{-1}$ and dwell time of 30 min. Results were expressed in terms of shrinkage (area %) as function of time [7,16].

RESULTS AND DISCUSSION

FIRING BEHAVIOUR

As expected, in all products water absorption decreases and the bulk density increased with the sintering temperature up to the maximum densification temperature (Fig. 1). Then, a decrease in the bulk density ascribed to a "bloating" effect (i.e., pore volume expansion), was detected.

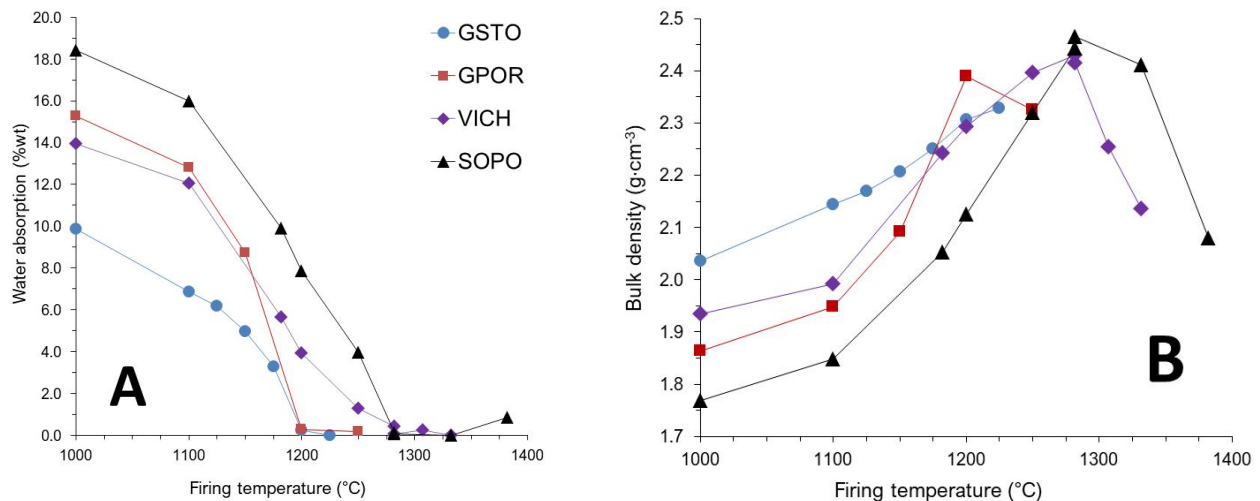


Fig. 1. Firing behaviour: water absorption (A) and bulk density (B).

In detail, the products reached the temperature of maximum densification (corresponding to the maximum value of bulk density) at 1200°C for GPOR, 1225°C for GSTO, and 1280°C for VICH and SOPO. The bulk density decrease observed at higher firing temperatures for GPOR, VICH and SOPO is attributable to the aforementioned "bloating".

It can be also observed that the different temperatures of maximum densification of the batches correspond to low water absorption values (<0.5%wt), as prescribed for each specific ceramic product.

PHASE EVOLUTION DURING FIRING

After firing at 1000°C, all bodies are composed of some residual amount of illite, K-feldspar, plagioclase and quartz; in addition, mullite and a non-crystalline matrix were formed (Fig. 2). Significant variations were observed with the increasing temperature :

Porcelain stoneware: as expected, feldspars melted quickly, while quartz was slowly dissolved; mullite, after its formation at about 1000°C, kept almost constant with a limited decrease; a non-crystalline matrix formed after breakdown of clay minerals and feldspars, and it grew rapidly with the temperature increase [7].

Glass-bearing stoneware: the plagioclase is substantially stable, given its slow melting, whilst quartz was dissolved more rapidly than the other phases; at 1100°C cristobalite formed and remained stable up to the highest firing temperature; the non-crystalline matrix was formed at a slower rate than that observed for GPOR.

Vitreous china and soft porcelain: feldspars were quickly melted up to 1200°C and quartz was partially dissolved above this temperature; abundant mullite was formed in the 1100-1200°C range, then underwent dissolution-precipitation at higher temperature, including the development of secondary mullite; the amount of non-crystalline matrix in the final products varied due to the above-mentioned melting and crystallization phenomena [17-18].

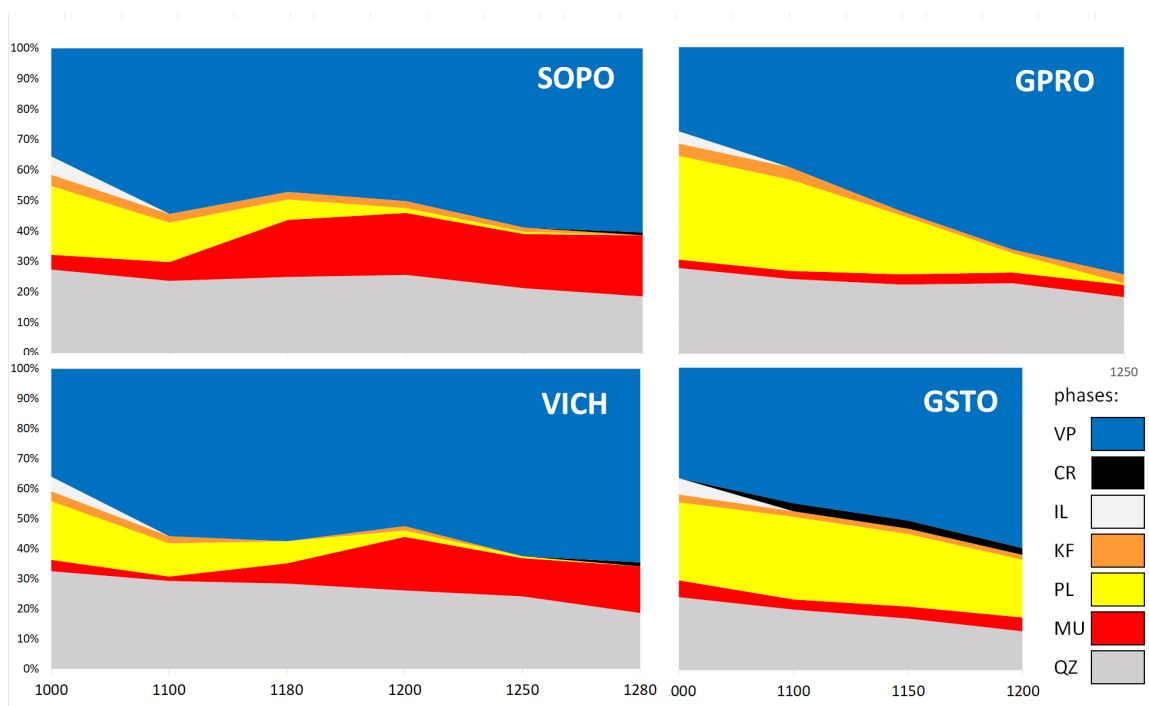


Fig. 2. Phase composition as a function of firing temperature for soft porcelain (SOPO), vitreous china (VICH), porcelain stoneware (GPOR), and glass-bearing stoneware (GSTO). Phase symbols: VP vitreous phase, CR cristobalite, IL illite, KF K-feldspar, PL plagioclase, MU mullite, QZ quartz.

COMPOSITION AND PROPERTIES OF THE NON-CRYSTALLINE MATRIX

The non-crystalline matrix changed its composition continuously with firing temperature due to the complex set of reactions involving residual and newly formed crystalline phases. Such variations are shown in Figure 3, by the degree of depolymerization in silicate melts (NBO/T), and the alumina saturation index (ASI).

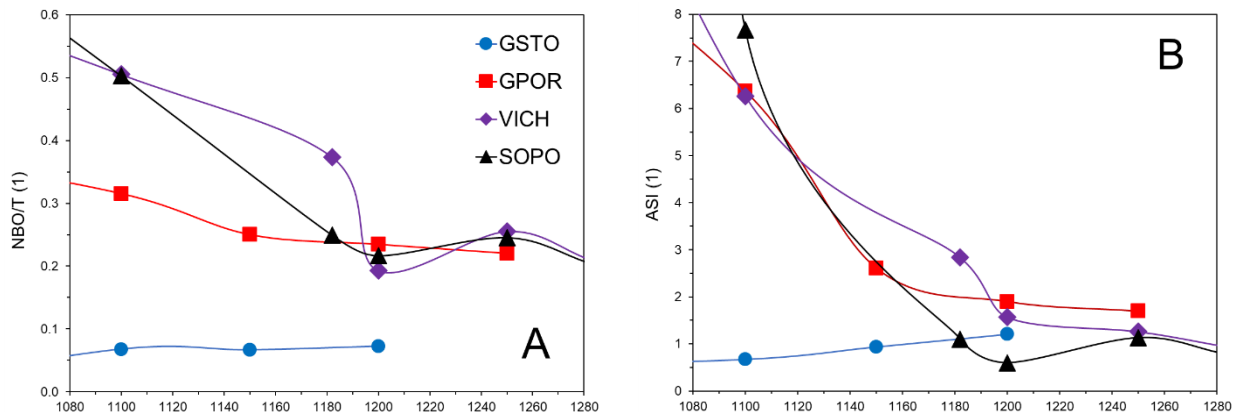


Fig. 3. Compositional and glass network connectivity parameters of the non-crystalline matrix as a function of the firing temperature: degree of depolymerization (A) and alumina saturation index (B).

The glass bearing stoneware is distinguished by lower values of NBO/T, hence a very high degree of polymerization (Fig. 3A). In the other batches, the liquid phase tends to be increasingly polymerized in all batches up to approximately 1200°C, as NBO/T decreases. For higher temperatures, the curves of GPOR, VICH and SOPO are almost superimposed and show no further changes of the glass network connectivity parameters.

Similar trends of GPOR, VICH and SOPO, decreasing up to 1200°C, are observed also for the ASI (Fig. 3B). These trends are mainly related to the crystallization of mullite, which acts as the main buffer for aluminium in the body. In countertrend with the other batches, GSTO exhibits low ASI values that slightly increase with temperature.

Such compositional features reflect the properties of the non-crystalline matrix in terms of shear viscosity and surface tension at high temperature (Fig. 4). In particular, the surface tension to shear viscosity ratio is related to the viscous flow sintering kinetics, since the higher is the ratio, the faster is the densification rate [7]. As expected, this ratio increases with the firing temperature in all samples, because the consequent viscosity drop is larger than the simultaneous surface tension reduction.

The effective viscosity (i.e., the viscosity of the bulk body accounting for the effect of solid particles on melt viscosity) decreases with the firing temperature with clearly distinct trends for porcelain and porcelain stoneware (Figure 4B). GPOR and GSTO effective viscosity reduction is steeper than that of VICH and SOPO. This is due to the formation of a more abundant and less viscous liquid phase in porcelain stoneware.

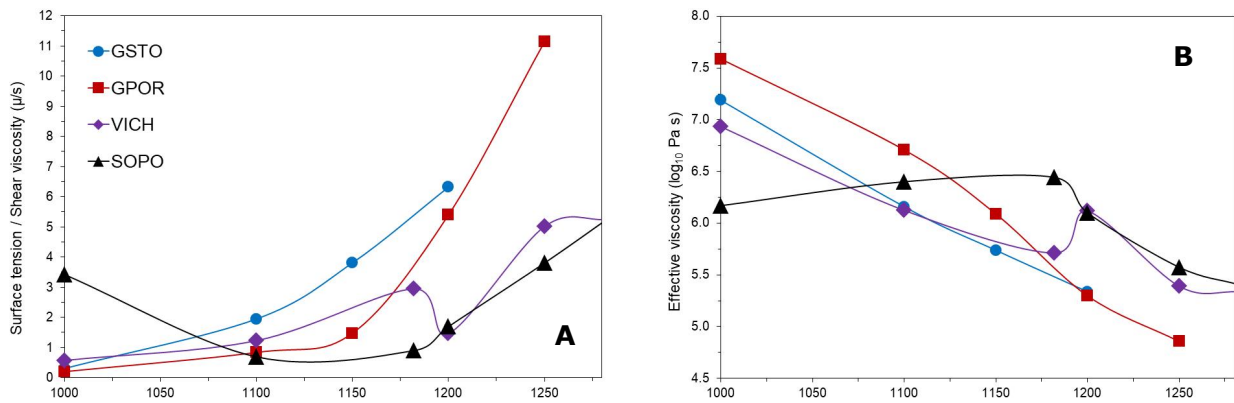


Fig. 4. Surface tension to shear viscosity ratio of the non-crystalline matrix (A) and effective viscosity of the bulk (B) as a function of firing temperature for soft porcelain (SOPO), vitreous china (VICH), porcelain stoneware (GPOR), and glass-bearing stoneware (GSTO).

SINTERING KINETICS

The densification kinetics is faster in the porcelain stoneware formulations than in soft porcelain and vitreous china. This can be appreciated, for instance, in the isothermal experiments at 1200°C (Fig. 5A) where the slope of GPOR is overlapped to GSTO but clearly steeper than those of VICH and SOPO, which are close to each other.

Taking into account the linear trend of the first sintering stage (down to about 10% of shrunk area), different sintering rates are calculated (Fig. 5B).

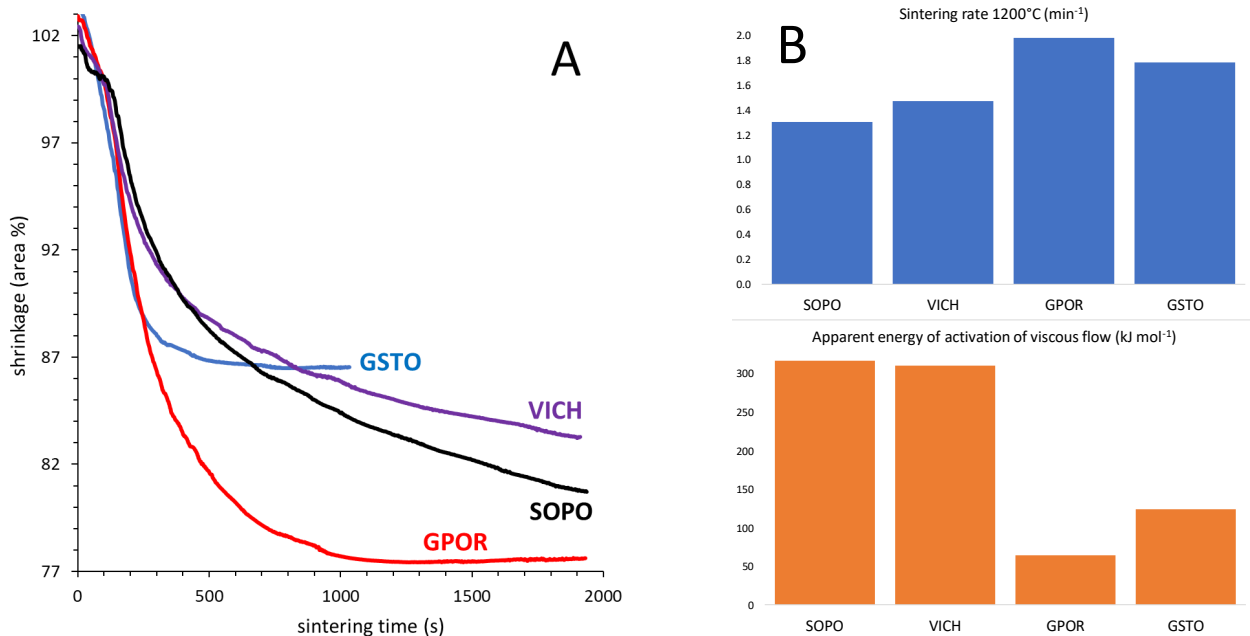


Fig. 5. Sintering kinetics at 1200°C (A); constant rates of sintering and apparent energy of activation of viscous flow (B) and for soft porcelain (SOPO), vitreous china (VICH), porcelain stoneware (GPOR), and glass-bearing stoneware (GSTO).

Although the sintering rates of stonewares are analogous, there is a significant difference in their densification efficiency: GPOR shrank much more than GSTO, which retained a larger volume of closed porosity. On the porcelain side, VICH and SOPO behave differently in the final sintering stage, although their very similar trends in the first stage. SOPO has a slightly slower sintering kinetics but a higher bulk density.

Overall, the lower is the apparent energy of activation of the viscous flow, the faster is the sintering rate. However, the ranking of Fig. 5A does not correspond to the final degree of densification. The glass-bearing stoneware has a low densification efficiency that is likely an effect of the composition of the GSTO non-crystalline matrix (a highly polymerized peralkaline melt). The porcelains are characterized by a prolonged final stage of sintering, which is probably due to the crystallization and growth of secondary mullite. This is somewhat reflected in the much higher effective viscosity of VICH and SOPO that prevents any dimensional deformation up to 1300°C.

CONCLUSIONS

Porcelain and porcelain stoneware, despite their compositional similarities, behave in a clearly different way during sintering. Such differences in firing behaviour are the convolution of a highly distinct phase evolution with its effects on the composition and structure of the non-crystalline matrix. Thus, 'porcelain' and 'porcelain stoneware' must not be confused with each other (the term 'porcelain tile' is misleading and should not be used).

The present study highlighted the fundamental role of the non-crystalline matrix, whose properties govern both the sintering kinetics and the densification efficiency. A detailed investigation is in progress on the relationship between compositional and glass network connectivity features of melts and technological performances.

Attention should be paid to the distinct role of mullite in porcelain and porcelain stoneware. This entails the different effects that primary and secondary mullite phases have during sinter-crystallization. It is crucial from the microstructural point of view in soft porcelain (SOPO) and vitreous china (VICH), as the growth of secondary mullite with a high aspect ratio ensures excellent mechanical strength. It is important in constraining the composition of the vitreous phase in porcelain stoneware (GPOR), since mullite acts as a buffer of aluminium.

REFERENCES

- [1] W. M. Carty and U. Senapati, Porcelain-raw materials processing, phase evolution and mechanical behavior. *J. Am. Ceramic Soc.* 81 (1998) 5-20.
- [2] Y. Iqbal, On the glassy phase in tri-axial porcelain bodies. *J. Pak. Mater. Soc.* 2 (2008) 62-71.
- [3] M. Romero, Relation between the microstructure and technological properties of porcelain stoneware. A review. *Materiales de construcción* 65 (2015) 2-16.
- [4] W. M. Carty and B. M. Pinto, Effect of filler size on strength of porcelain bodies. *Ceram. Eng. Sci. Proc.* 23 (2002) 95-105.
- [5] J. M. Perez and M. Romero, Microstructure and technological properties of porcelain stoneware tiles moulded at different pressures and thicknesses. *Ceram. Int.* 40 (2014) 1365-1377.
- [6] C. B. Becker, W. Carty, E. Schillinger, The effect of sodium/potassium ratio on melting in triaxial porcelain. *Ceram. Eng. Sci. Proc.* 20 (1999) 43-51.
- [7] S. Conte, C. Zanelli, M. Ardit, G. Cruciani, M. Dondi, Phase evolution during reactive sintering by viscous flow: disclosing the inner workings in porcelain stoneware firing. *J. Eur. Ceram. Soc.* 40 (2020) 1738-1752.
- [8] M. J. Jackson, B. Mills, Dissolution of quartz in vitrified ceramic materials, *J. Mater. Sci.* 32 (1997) 5295-5304.
- [9] B. H. Toby, EXPGUI, a graphical user interface for GSAS. *J. Appl. Crystallogr.* 34 (2001) 210-213.
- [10] A. C. Larson, R. B. Von Dreele, GSAS, General Structure Analysis System, Los Alamos National Laboratory, Los Alamos, NM, (1988) 86-748.
- [11] A. F. Gualtieri, V. Riva, A. Bresciani, S. Maretta, M. Tamburini, A. Viani, Accuracy in quantitative phase analysis of mixtures with large amorphous contents. The case of stoneware ceramics and bricks. *J. Appl. Crystallogr.* 47 (2014) 835-846.
- [12] D. Giordano, J. K. Russell, D. B. Dingwell, Viscosity of magmatic liquids: a model. *Earth Planet. Sc. Lett.* 271 (2008) 123-134.
- [13] A. A. Appen, "Chemistry of Glass (Russ.)". *Khimiya: Leningrad, Russia*, (1974) 351.
- [14] A. Dietzel, Relation between the surface tension and the structure of molten glass. *Kolloid-Z.* 100 (1942) 368-380.
- [15] I. M. Krieger, T. J. Dougherty, A mechanism for non-Newtonian flow in suspensions of rigid spheres. *J. Rheol.* 3 (1959) 137-152.
- [16] S. Conte, C. Zanelli, M. Ardit, G. Cruciani, M. Dondi, Predicting viscosity and surface tension at high temperature of porcelain stoneware bodies: a methodological approach. *Materials* 11 (2018) 2475.
- [17] N. Marinoni, A. Pagani, I. Adamo, V. Diella, A. Pavese, F. Francesconi, Kinetic study of mullite growth in sanitary-ware production by in situ HT-XRPD. The influence of the filler/flux ratio. *J. Eur. Ceram. Soc.* 31 (2011) 273-280.
- [18] W. E. Lee, G. P. Souza, C. J. McConville, T. Tarvornpanich Y. Iqbal, Mullite formation in clays and clay-derived vitreous ceramics. *J. Eur. Ceram. Soc.* 28 (2008) 465-471.